Effects of physical, chemical, and biological ageing on the mineralization of pine wood biochar by a *Streptomyces* isolate

Nayela Zeba, Timothy D. Berry, Thea L. Whitman*

Department of Soil Science, University of Wisconsin-Madison, Madison, WI, 53703, USA

*Email: twhitman@wisc.edu

Abstract

If biochar is to be used for carbon (C) management, we must understand how ageing affects biochar C mineralization. Here, we incubated aged and unaged eastern white pine wood biochar produced at 350 and 550 °C with a *Streptomyces* isolate, a putative biochar-decomposing microbe. Ageing was simulated via exposure to (a) alternating freeze-thaw and wet-dry cycles (physical ageing), (b) concentrated hydrogen peroxide (chemical ageing) and (c) nutrients and microorganisms (biological ageing). Elemental composition and surface chemistry (Fourier Transform Infrared spectroscopy) of biochar samples were compared before and after ageing. Ageing significantly increased biochar C mineralization in the case of physically aged 350 °C biochar ($p < 0.001$). Among 350 °C biochars, biochar C mineralization was positively correlated with an increase in O/C ratio ($R^2 = 0.78$) and O-containing functional groups ($R^2 = 0.73$) post-ageing, suggesting that surface oxidation during ageing enhanced biochar degradation by the isolate. However, in the case of 550 °C biochar, ageing did not result in a significant change in biochar C mineralization ($p > 0.05$), likely due to lower surface oxidation and high condensed aromatic C content. These results have implications for the use of biochar for long term C storage in soils.

Synopsis: This study highlights the impact of ageing on the microbial mineralization of biochar, which can affect its long-term C storage capacity.

Keywords: Aging, Biochar C mineralization, FT-IR, Surface oxidation, O/C ratio, pyrogenic C, PyC, pyrogenic organic matter, PyOM

29 **TOC Graphic**

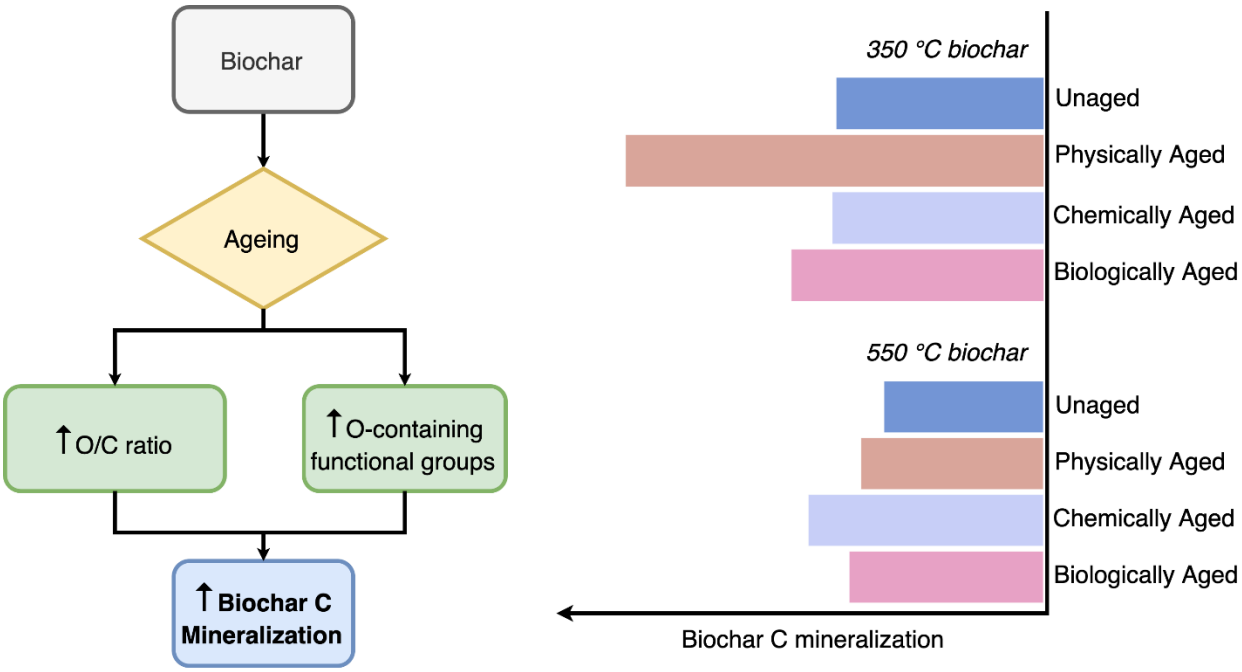

30

1. Introduction

Biochar is the carbon-rich solid product of pyrolysis, the process of heating biomass under oxygen limited conditions [1]. Biochar has the potential to be used as a soil amendment for agricultural management (e.g., to increase water holding capacity, among other effects) and as a carbon (C) management strategy to help mitigate greenhouse gas emissions [2]. Converting waste biomass into biochar can potentially be an effective way to sequester C, since the C contained in biochar is generally more resistant to mineralization compared to the C in the parent biomass [2,3], although the net C effects of biochar production and soil application depend heavily on system-specific parameters, particularly the baseline scenario for the fate of the parent biomass [4–7].

Biochar C is resistant to mineralization primarily because of its high proportion of condensed aromatic C [2,8,9], which has been shown to be resistant to mineralization by both abiotic and biotic processes [10,11]. Further, biochar, while being rich in C, tends to have a low oxygen (O) content, and low O/C ratios in biochar have been shown to correlate with biochar persistence in soil [12]. The chemical and physical properties of biochar that affect its persistence are initially determined by the production conditions, such as feedstock and production temperature [13], but once the biochar is deposited in soil, these properties change over time in a process known as ageing [14–17]. Natural ageing of biochar in soil is a complex process [14], with multiple relevant mechanisms. We focus on three of these dominant mechanisms over the course of this paper:

1. *Physical ageing* - physical breakdown of biochar, primarily by freeze-thaw cycles and changes in temperature and moisture [14,18–20]
2. *Chemical ageing* - degradation of biochar through abiotic oxidation upon exposure to various oxidizing agents [21–23]

3. *Biological ageing* - biotic degradation and corresponding physical and chemical modifications of biochar by microbes and other soil organisms [24–28]

Commonly reported effects of biochar ageing include a drop in pH, an increase in O content, and an increase in O-containing functional groups on the surface of aged biochar compared to unaged biochar. This suggests that ageing of biochar, both naturally and artificially, causes changes to its elemental composition and surface chemistry [17]. Furthermore, these changes have been shown to affect properties of biochar such as sorption [18,29] and cation exchange capacity [30,31]. However, we still have limited information on how these changes will affect soil CO_2 emissions and the decomposability of biochar itself. Spokas [32] reported an increase in total C mineralization upon incubation of soil amended with 3 year aged woody biochar, primarily due to chemical oxidation of biochar surfaces. On the other hand, Liu *et al*. [33] observed lower total C mineralization in soil incubations amended with 6 year aged wheat straw biochar due to loss of easily mineralizable C during ageing. The specific effects of ageing on the decomposability of biochar by soil microbes have not been fully explored [34].

Further investigating the relationship between physicochemical changes and biochar decomposability is one of the primary tranches of this work. Specifically, the aim of this study is to examine the decomposability of aged biochar by a specific biochar decomposing microbe from a genus that is common to soils worldwide – a *Streptomyces* isolate. We predicted that the change in mineralization with ageing will depend on whether the ageing process results in loss of easily mineralizable C (as indicated by aliphatic chemical groups), which would lead to lower

mineralization, or an increase in O content (as indicated by O/C ratios), which would lead to higher mineralization.

2. Materials and Methods

2.1. Production of biochar

Biochar was produced from eastern white pine wood chips (*Pinus strobus* (L.)) at highest treatment temperature (HTT) 350 and 550 °C in a modified Fischer Scientific Lindberg/Blue M Moldatherm box furnace (Thermo Fisher Scientific, Waltham, MA, USA) under continuous argon flow (1 L min^{-1}) and a residence time of 30 min [35]. Pyrolyzed material was ground using a ball mill and sieved to collect biochar with particle size <45 μm. The full details of biochar production can be found in Supplemental Note S1.

2.2. Ageing of biochar

Biochar produced at both 350 and 550 °C was subjected to one of three different ageing processes - physical, chemical and biological. We performed all ageing treatments on single batches of biochar to give us a final set of physically, chemically and biologically aged chars produced at 350 °C (350PHY, 350CHEM and 350BIO) and 550 °C (550PHY, 550CHEM and 550BIO). A batch of 350 °C unaged biochar (350UN) and 550 °C unaged biochar (550UN) acted as controls in our study.

Physical ageing

For physical ageing (PHY), we subjected biochar samples to 20 freeze-thaw-wet-dry cycles between -80 °C and 100 °C using pint-sized Mason jars (473.18 mL), building on the method

reported by Hale *et al.* [18]. We chose this wide temperature range based on findings by Cheng *et al.* [14] that demonstrated that ageing of biochar can occur over a temperature range from -22 °C to 70 °C and that greater ageing occurs at higher temperatures. Our method simulates an extreme scenario of severe weathering of biochar likely to occur across many seasonally snow-covered ecosystems in the northern hemisphere during precipitation-drying cycling and freeze-thaw cycling [36,37]. Quartz sand (Sargent Welch, Buffalo Grove, IL, USA) was used to simulate a soil matrix (80 g with a 5% weight biochar amendment) and ultrapure water was added to the jars containing 4 g of biochar to achieve 40% water holding capacity (WHC). During each cycle, the jars were frozen at -80 °C for a median time of 7 hours (min 5 h – max 48 h), thawed for a period of 1-2 hours, following which they were dried in the oven at 100 °C for a median time of 18 hours (min 14 h – max 54 h) and cooled to room temperature for a period of 1-2 hours. After each drying period, masses of the jars were measured, and ultrapure water was added to reach 40% WHC. After 20 cycles, biochar particles were separated from the sand by wet sieving using a US mesh size no. 270 sieve that allowed the biochar particles less than 45 μm in size to pass through while retaining the sand particles.

Chemical ageing

For chemical ageing (CHEM), we treated biochar samples with H_2O_2 based on the method reported by Huff and Lee [21]. We used a high concentration of H_2O_2 based on findings from previous studies that reported maximum changes in surface chemistry of biochar upon treatment with 30% w/w H_2O_2 solution [21,38]. Briefly, 30% w/w H_2O_2 solution was added to 5 g of biochar at a ratio of 1 g biochar : 20 mL solution and shaken inside a chemical fume hood for 2 hours at 100 rpm. After 2 hours of shaking, we filtered the biochar samples through sterile Whatman glass

122 microfiber filters (Grade 934-AH Circles – 1.5 µm particle retention) and rinsed with 100 mL
123 aliquots of ultrapure water to remove any residual H_2O_2.
124
125 *Biological ageing*
126 For biological ageing (BIO), we exposed the biochar samples to a microbial community in a
127 nutrient solution supplemented with glucose (40 µg glucose mg^{-1} biochar C), building on the
128 method reported by Hale *et al.* [18]. By adding glucose, we hoped to stimulate microbial activity and,
129 with it, the decomposition of biochar. We chose a microbial community expected to be enriched
130 in microbes that could degrade biochar to further accelerate the biological ageing treatment. We
131 derived the microbial inoculum from soil samples collected at the Blodgett Forest Research Station
132 at University of California, Berkeley, which has been used to conduct multiple prescribed burn
133 studies [39]. The soil samples for the inoculum were collected from 0-10 cm depth at the center of a
134 slash pile burn after removing the ash layers. To extract the inoculum, we mixed the field-moist
135 soil samples with Millipore water in sterile 50 mL centrifuge tubes and vortexed for 2 hours at
136 high speed. After vortexing, the tubes were allowed to stand for 5 minutes and the soil suspensions
137 were filtered through sterile 2.7 µm Whatman membrane filters into sterile centrifuge tubes. For
138 the biological ageing process, nutrient solution was prepared from autoclave-sterilized modified
139 basal salt solution (500 mL L^{-1} final biochar nutrient media), modified from Stevenson *et al.* [40],
140 filter-sterilized vitamin B12 solution (200 µL L^{-1} final biochar nutrient media), filter-sterilized
141 vitamin mixture (200 µL L^{-1} final biochar nutrient media) and a filter-sterilized trace element
142 solution (1 mL L^{-1} final biochar nutrient media) [41]. The detailed composition of the nutrient
143 solution is provided as supplementary material accompanying this work (Supplemental Note
144 S2.1.). We combined 5 g of biochar and glucose supplement (40 µg mg^{-1} biochar carbon) with 250

mL ultrapure water and autoclave-sterilized the mixture. After autoclaving, the biochar mixture was transferred to a quart-sized (946.35 mL) Mason jar and combined with 250 mL of the nutrient solution. Note that the pH of the modified basal salt solution, which is a part of the nutrient solution was adjusted to 7 to obtain a pH neutral final biochar nutrient media (Supplemental Note S2.1.). To the resulting biochar and glucose supplemented nutrient media, we added 8 mL of the filtered inoculum and incubated the jars at 30 °C in a shaker incubator set to 100 rpm for a period of 2 weeks.

2.3. Chemical Analyses

Total C and N were determined for aged and unaged biochar samples using a Thermo Scientific Flash EA 1112 Flash Combustion Analyzer (Thermo Fisher Scientific, Waltham, MA, USA) at the Department of Agronomy, UW- Madison, WI, USA. Total H was determined using a Thermo Delta V isotope ratio mass spectrometer interfaced to a Temperature Conversion Elemental Analyzer (Thermo Fisher Scientific, Waltham, MA, USA) at the Cornell Isotope Laboratory, NY, USA. Total O was calculated by subtraction as per Enders *et al.* [13], after determining ash content of aged and unaged biochar samples using the method prescribed by ASTM D1762-84 Standard Test Method for Chemical Analysis of Wood Charcoal (See further details in Supplemental Note S1).

The pH of aged and unaged biochar samples was measured in deionized water at a 1:20 solid: solution ratio using an Inlab Micro Combination pH electrode (Mettler Toledo, Columbus, OH, USA) connected to a Thermo Scientific Orion Star A111 benchtop pH meter (Thermo Fisher

Scientific, Waltham, MA, USA). Further details of this procedure can be found in the Supplemental Note S1.

The FT-IR measurements were performed at the U.S. Dairy Forage Research Center, Madison, WI, USA with a Shimadzu IRPrestige-21 FT-IR spectrometer (Shimadzu, Kyoto, Japan) on the ATR (Attenuated Total Reflection) absorbance mode. Briefly, 5-10 mg of the biochar sample was placed on the Zn-Se sample trough and scanned. For each sample, we obtained 256 scans per sample in the range from 4000 to 650 cm^{-1} with a resolution of 1 cm^{-1} (550UN, 350PHY and 550PHY) and 2 cm^{-1} (350CHEM, 550CHEM, 350BIO, 550BIO and 350UN). Background corrections were performed between each sample measurement. We assigned wavenumbers for selected functional groups based on previous studies (S.I. Table S1) and quantified the peak heights of selected functional groups after spectrum normalization using the Shimadzu IR Solution FT-IR software (S.I. Table S2). Fractional signal heights for each of the FT-IR peaks were calculated by dividing the signal height of each of the peaks by the sum total of signal heights of all peaks of interest to determine the contribution of the signal generated by a particular species to the full spectra. Further details of this procedure can be found in the Supplemental Note S1.

Multivariate comparisons: To compare the full FT-IR spectra of biochar samples across temperatures and different ageing treatments, we used a multivariate dendrogram technique. We used the continuous normalized data for these analyses, excluding the region from 4000 cm^{-1}- 3100 cm^{-1} wavenumber to remove signals from water sorbed to the biochar surface. We used the dendextend [42] package in R to construct a dendrogram. Euclidean distances between biochar samples were calculated using the dist() function, and the hclust() function with the complete

190 linkage method used for hierarchical clustering, where the two most similar samples are clustered
191 together, one after another, forming an ordered hierarchical tree/ dendrogram.
192
193 **2.4. Incubation**
194 We performed the incubations with all the aged biochar (PHY, CHEM and BIO) as well as
195 unaged biochar (UN) produced at both 350 and 550 °C as solid agar biochar media, inoculated
196 with a bacterial isolate known to grow on biochar, while tracing CO_2 emissions from each
197 replicate.
198
199 The bacterial isolate we used was a *Streptomyces* that was isolated on media with eastern white
200 pine wood biochar produced at 500 °C as the sole C source. The primary motivation for selecting
201 this specific species is that it was able to grow on biochar media during trial lab incubations.
202 Further, there is evidence that indicates that bacterial genera that respond positively to biochar
203 addition in soils include members that have the potential to break down polycyclic aromatic
204 hydrocarbons (PAHs) [43], a constituent of biochars, particularly high-temperature ones. We
205 recovered the isolate from glycerol stocks by streaking onto a biochar (produced from pine wood
206 at 350 °C) nutrient media agar plate (as described in Supplemental Note S2.) and incubating for 5
207 days at 37 °C. A single colony from the biochar media plate was inoculated into 30 g L^{-1} Tryptic
208 soy broth (Neogen Culture Media, Lansing, MI, USA) and incubated at 30 °C in a shaking
209 incubator until growth was visible, characterized by turbidity in the media.
210
211 We performed incubations in quarter-pint sized Mason jars (118.29 mL). Biochar (1 g L^{-1} final
212 biochar nutrient media) and Noble agar suspension (30 g L^{-1} final biochar nutrient media) were

sterilized by autoclaving and combined with nutrient solution to obtain a pH neutral final biochar nutrient media (Supplemental Note S2.). For each sample, we poured 40 mL of the final biochar nutrient media into sterile Mason jars. After the agar solidified, 20 µL of the bacterial suspension in malt extract broth was plated onto the agar surface using the spread plate technique [44].

We performed the incubations in replicates of at least three for each treatment and included uninoculated controls for each treatment. In addition, we included two empty jars as gas flux blanks for the experiment. After plating, the jars were capped and sealed with sterile, gas-tight lids provided with fittings that facilitate CO_2 gas measurements and attached to randomly selected positions on the distribution manifolds (multiplexer) using polyurethane tubing [45]. We measured the concentration of CO_2 respired in the headspace of each jar at intervals of 3-4 days using a Picarro G2131i cavity ringdown spectrometer attached to the multiplexer over a period of 1 month. After each measurement, we flushed the jars with a 400 ppm CO_2-air gas mixture to ensure aerobic conditions inside the jar. The precise concentration after flushing each jar was measured and subtracted from the next time point reading to determine the respired CO_2 in the jar. From previous biochar incubation trials with the isolate, we confirmed that sampling over a 3-4-day interval did not lead to hypoxia inside the jars.

The raw CO_2 readings measured using the multiplexer-Picarro system were processed in R to calculate biochar C mineralized over the period of incubation using the following packages: tidyverse [46], zoo [47], RColorBrewer [48], and broom [49]. Briefly, we calculated the cumulative biochar C mineralized for each replicate at each time point. We corrected the cumulative biochar C mineralized values for all replicates by subtracting the corresponding mean C mineralized of

uninoculated replicates within each treatment and a time series was plotted comparing the biochar C mineralization trends between the aged and unaged biochar samples.

Data Analysis / Statistical Methods:

We performed most calculations in R using the packages dplyr [50] and tidyr" [51]. Figures were made using the ggplot2 [52] and wesanderson [53] packages and all code used for analyses and figures in this paper is available at github.com/nayelazeba/biochar-ageing.

We performed ANOVA and Tukey's HSD test in R to compare significant differences between cumulative biochar C mineralized across all aged and unaged biochar treatments for both 350 °C and 550 °C biochar. In order to correlate total C mineralized during the one-month incubation period across all aged and unaged biochar samples with fractional signal heights of each of the selected functional groups and molar O/C ratios, we performed linear regressions in R.

Microbial growth

After the incubation period, we disconnected the jars and analyzed images of the agar surfaces using the software *ImageJ* [54]. The percentage area occupied by the growth of bacterial colonies was determined for each incubation jar and used as a rough proxy to compare microbial growth between jars (S.I. Fig. S1).

3. Results and Discussion

3.1. Effect of ageing on elemental composition

Aged biochars produced at both 350 °C and 550 °C had lower total C and higher total O contents than unaged biochar, except in the case of 350CHEM, where we did not observe similar trends (Table 1). The molar O/C ratio increased for 350BIO (0.26) and was highest for 350PHY (0.39) compared to 350UN (0.20) among 350 °C chars. In the case of 550 °C chars, the O/C ratio increased for 550BIO (0.18), 550PHY (0.15) and was highest for 550CHEM (0.26) compared to 550UN (0.11). This is consistent with previous studies that have shown an increase in O/C ratio following natural as well as artificial ageing of biochar through abiotic and biotic processes [14,19,20,30,55]. The relative decrease in C with ageing is likely due in part to leaching of C-rich dissolved organic matter [19]. Additionally, abiotic oxidation of C to carbon dioxide and utilization of C as a substrate by microbes in the case of biologically aged biochars is likely to result in relatively greater loss of C than O [10,24,30,56]. The higher O content in aged biochars indicates an increase in O-containing functional groups that is likely due to both abiotic oxidation of C in the case of chemically and physically aged biochars [14,30] as well as microbially mediated oxidation in the case of biologically aged biochars [55]. The effects of pyrolysis temperature on the elemental composition of biochar are discussed in Supplemental Note S4.

Table 1. Elemental Composition, Elemental Ratio, and pH of the Unaged and Physically, Chemically and Biologically aged biochar samples produced at low temperature (350°C) and high temperature (550 °C)*

HTT (°C)	Ageing treatment	Total C	Total N	Total H	Ash	Derived total O	O/C	pH in solution
		(wt %)						
350	Unaged	75 ± 0.04	0.3 ± 0.00	3.9 ± 0.01	0.6 ± 0.02	20.4	0.20	6.1 ± 0.1
	Physical	61 ± 1.03	0.3 ± 0.1	2.7 ± 0.04	4.3 ± 0.01	31.8	0.39	3.3 (N = 1)
	Chemical	80 ± 4.6 (N = 4)	0.3 ± 0.04 (N = 4)	2.5 ± 0.2	1.6 ± 0.04	15.6	0.15	4.3 ± 0.02
	Biological	70 ± 1.2	0.3 ± 0.01	3.5 ± 0.2	1.8 ± 0.2	24.4	0.26	4.8 ± 0.06
550	Unaged	85 ± 1.2 (N = 4)	0.2 ± 0.02 (N = 4)	2.4 ± 0.2	0.8 ± 0.03	11.9	0.11	6.9 ± 0.08
	Physical	79 ± 0.1	0.4 ± 0.02	2.2 ± 0.01	3.1 ± 0.2	15.8	0.15	6.5 (N = 1)
	Chemical	71 ± 0.2	0.3 ± 0.02	3.8 ± 0.4	0.7 ± 0.05	24.4	0.26	5.0 ± 0.2
	Biological	77 ± 3.7	0.3 ± 0.01	2.5 ± 0.1	2.4 ± 0.1	18.2	0.18	4.8 ± 0.6 (N = 4)

*Note: Data shown represent the mean ± standard deviation based on duplicate measurements unless specified otherwise. While ageing caused changes in pH (See Supplemental Note S3 for discussion), we controlled for the effects of pH on microbial activity in this study by adjusting the pH of the final nutrient biochar media for all samples.

3.2. Effect of ageing on surface chemistry

Amongst the ageing treatments, physical ageing altered the surface chemistry of biochar the most (Fig. 1). For both 350 °C and 550 °C biochar samples, the spectra of physically aged biochar samples were the most dissimilar from the spectra of unaged biochar samples. While chemical and biological ageing also caused changes to surface chemistry, the effects appear to be less pronounced than in the case of physical ageing, as we see these samples cluster together more by production temperature than treatment method – *i.e.*, production temperature was a more important determinant of biochar chemistry than ageing treatment. An important factor driving dissimilarity between 350 °C and 550 °C biochars is the increase in aromatic carbon content and decrease in H and O-containing functional groups on the surface of biochar with increasing pyrolysis temperatures [10,11,57] (See Supplemental Note S4 for further discussion on effects of pyrolysis temperature on surface chemistry). It is interesting to note that the two PHY aged samples are more similar to each other than to other samples produced at the same pyrolysis temperatures. This suggests that the physical ageing treatment had a stronger effect on the surface chemistry than production temperature.

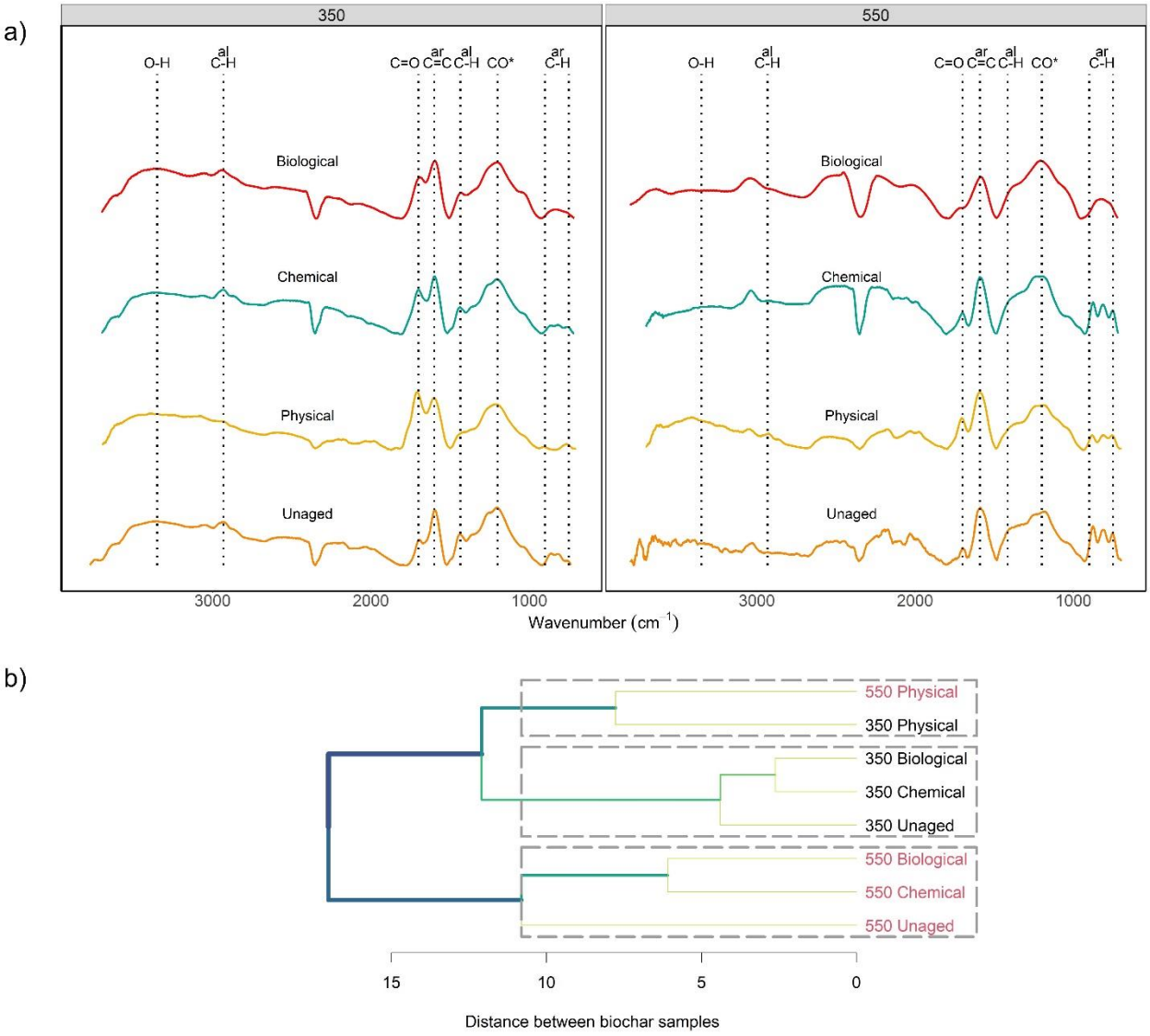

Figure 1. (a) FT-IR spectra of unaged and physically, chemically and biologically aged biochar samples produced at 350 °C (left panel) and 550 °C (right panel). Labels on top indicate the peak names assigned to different functional groups as described in detail in supplementary information (O-H: O–H stretching of carboxylic acids, phenols, alcohols at 3370 cm^{-1}; al CH: aliphatic C-H stretch of CH_3 and CH_2 at ~2932 cm^{-1} and C-H bending of CH_3 and CH_2 at 1413 cm^{-1}; C=O: C=O stretch in carboxylic acids and ketones at ~1701 cm^{-1}; ar C=C: aromatic C=C vibrations and stretching of quinones at ~1593 cm^{-1}; CO*: C–O stretching, O–H bending of COOH and/or C–OH stretching of polysaccharides at ~1200 cm^{-1}; ar C-H: aromatic C-H out of plane deformation at 810

305 cm^{-1}. **(b)** The clustering of biochar FT-IR spectra based on Ward's hierarchical clustering method
306 represented as a dendrogram. The distance of the link between any two clusters (or samples) is a
307 measure of the relative dissimilarity between them.

308

309 *Surface oxidation:* An important feature that stood out when comparing the FTIR spectra of
310 unaged and aged biochars was the increase in O-containing carboxylic groups, measured by
311 changes in the relative peak height of the C=O stretch at 1701 cm^{-1} wavenumber (Fig. 1a and S.I.
312 Table S2). Physically aged biochar across pyrolysis temperatures showed the maximum values for
313 C=O stretch, indicating that the surfaces of physically aged biochar were the most oxidized and
314 rich in carboxylic groups. Chemical ageing also resulted in surface oxidation. We measured a
315 slight increase in carboxylic groups for both 350 °C and 550 °C chemically aged chars compared
316 to unaged chars. The increase in surface oxygenation and O-containing functional groups after
317 ageing is consistent with the findings of previous studies that investigated changes in surface
318 chemistry using methods analogous to the physical and chemical treatments used in this study [14,19–
319 22]. For biological ageing, surface oxidation was observed only in the case of 350BIO. We did not
320 observe any increase in the relative peak height of carboxylic groups in the case of 550BIO
321 compared to 550UN. This suggests that abiotic oxidation through physical and chemical ageing
322 methods used in the study resulted in more surface oxidation and carboxylic groups compared to
323 biotic oxidation through biological ageing. This agrees with the finding of Cheng *et al.* [30], where
324 they noted that abiotic processes were more important than biotic processes for the initial surface
325 oxidation of fresh biochar. Our observations indicate that 350 °C biochars were more oxidized
326 compared to 550 °C chars within a given ageing treatment (Fig. 1a and S.I. Table S2). This is most
327 likely due to higher aromatic carbon content in biochar produced at 550 °C that tends to be more

condensed and resistant to oxidation while the 350 °C chars have low aromatic carbon content that is less condensed and amorphous and more likely to undergo oxidation [10,11]. This has been confirmed by other studies that observed an increase in resistance to oxidation by biochar produced at higher pyrolysis temperatures [38,58,59].

Surface aromatic and aliphatic groups: When considering how ageing affected the surface aromatic and aliphatic groups, we found that pyrolysis temperature was an important factor controlling these changes. For 350 °C biochars, we consistently observed a decrease in relative peak height in the 1413 cm^{-1} aliphatic C-H stretch, 810 cm^{-1} aromatic C-H stretch and 1593 cm^{-1} C=C aromatic stretch regions after ageing. The maximum decrease in peak values was consistently observed for 350PHY. Additionally, in the case of 350PHY, we measured a considerable decrease in relative peak height for the aliphatic C-H stretch at 2932 cm^{-1} after ageing. In the case of 550 °C char, we observed a considerable decrease in the relative peak height for the aromatic C-H stretch and a slight decrease in the 1413 cm^{-1} aliphatic C-H stretch after ageing but the same was not observed in the case of the C=C aromatic stretch. These changes indicate a relative loss or transformation of both surface aliphatic and aromatic carbon groups during ageing. As discussed earlier, the loss in C could be due to leaching or abiotic oxidation of C during ageing. Further, in the case of biological ageing, the relative loss in aliphatic C group at 1413 cm^{-1} and 2932 cm^{-1} (for 350°C chars) could be a result of decomposition of aliphatic C by soil microbes [24,25,60]. While it may not be possible to conclusively determine whether oxidized functional groups were previously associated with aromatic vs. aliphatic compounds, the drop in relative heights in the aromatic regions (810 and 1593 cm^{-1} wavenumbers) accompanied by a relative increase in signal for carboxyl (1701 cm^{-1}) group suggests that the oxidation of aromatic C results in the development

of carboxylic groups. It has been previously suggested that oxidation on the edges of the aromatic backbone of biochar, taking place over a long period of time, could lead to the formation of negatively charged carboxyl groups [56,61,62]. A loss in aromatic functional groups was documented during physical ageing of peanut straw biochar [20] and during chemical ageing of pine wood biochar [21]. More recently, Yi *et al.* [63] measured loss and transformation of condensed aromatic C after 9 years of field ageing of high temperature bamboo and rice straw biochar. These previous findings support the inference that ageing methods used in this study could have caused the disruption of aromatic carbon to form carboxylic groups.

It is important to note that FTIR spectra as produced and analyzed in this study are only semi-quantitative – *i.e.*, a doubling in peak height does not necessarily represent twice as much of the bond associated with that wavenumber. Furthermore, since replicates for ageing treatments and FTIR measurements were not included, we cannot determine whether these differences are statistically significant. However, the spectra represent an average of 265 scans on pooled and homogenized samples, and consistent responses to ageing at the two different temperatures as well as consistent temperature effects across different ageing treatments both help give us confidence in the trends observed here.

3.3. Effect of ageing on biochar C mineralization

The biochar C mineralization trends for all treatments show a similar pattern overall, with an initial period of steep increase in C mineralization, followed by the onset of a period of lower C mineralization (about 350 hours after the start of incubation, Fig. 2). This is comparable to the C mineralization curves commonly observed in previous incubation studies with soil amended with

374 biochar [28,33,64,65] and biochar inoculated with a microbial community from a forest soil [60,66,67].
375 Cumulative biochar C mineralized was significantly higher for 350 °C biochars compared to 550
376 °C biochars (Tukey test, $p_{adj} = 0.003$). This is consistent with previous studies that have noted
377 higher microbial activity and respiration in incubations with low temperature chars [56,67–69], since
378 biochar produced at high pyrolysis temperature contains a larger fraction of condensed aromatic
379 C, which is more difficult for microorganisms to oxidize [11,58,70–72]. Growth on agar surfaces over
380 the month-long incubation, as measured by total surface area, was higher for 350 °C biochar
381 treatments as compared to their 550 °C counterparts (S.I. Fig. S2). This corresponds to trends
382 observed in the cumulative biochar C mineralized over the incubation period, indicating that the
383 *Streptomyces* strain more effectively colonizes and grows on agar surfaces containing biochar
384 particles produced at 350 °C.
385

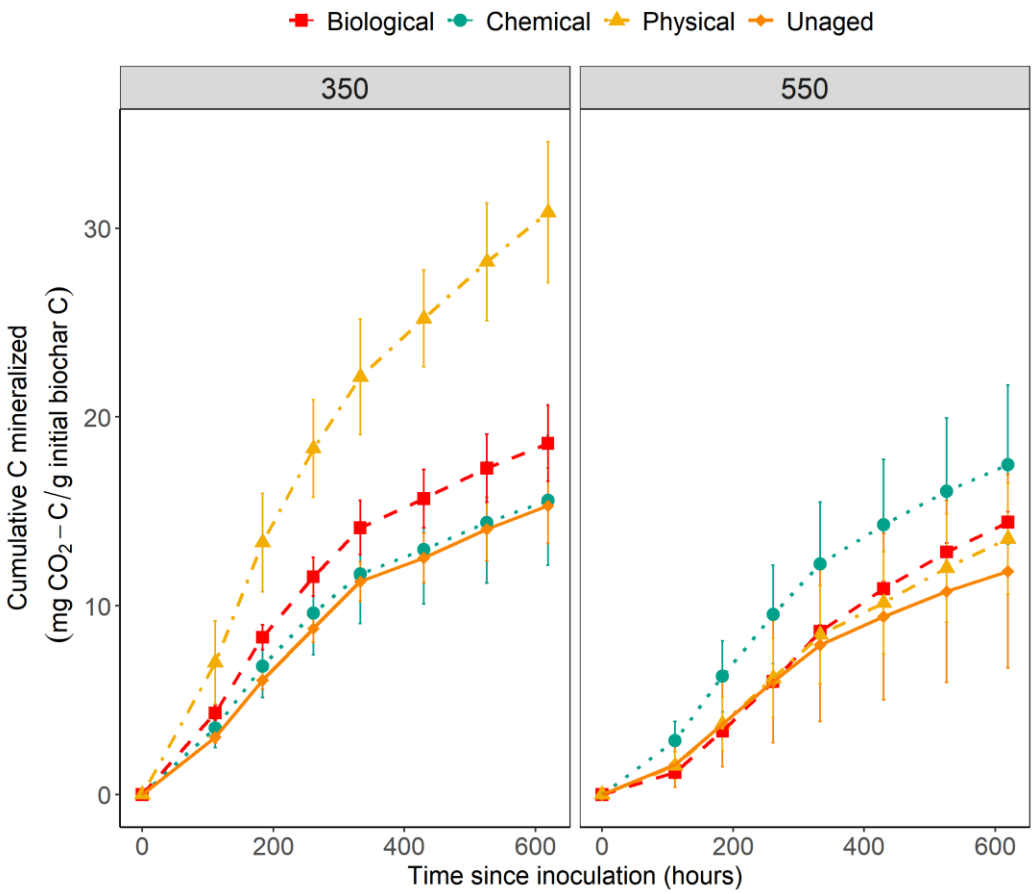

386

387 **Figure 2.** Mean cumulative C mineralized from unaged and physically, chemically and
388 biologically aged biochar samples over time, with uninoculated blanks subtracted and normalized
389 with mean biochar-C. N=3 for physical, chemical and unaged, N=5 for biological. Error bars
390 represent 95% confidence intervals. The left panel shows biochars produced at 350 °C and the
391 right panel shows biochars produced at 550 °C.

392

393 Amongst the 350 °C chars, the cumulative biochar C mineralized for aged biochars was higher
394 than that for unaged biochar through the entire incubation period (Fig. 2), although the difference
395 in C mineralization was statistically significant only in the case of 350PHY (Tukey test, p_{adj} =

396 0.0001). 350PHY treatments also showed the greatest surface growth (S.I. Fig. S2), consistent with
397 the cumulative biochar C mineralized data.
398
399 Amongst the 550 °C biochars, there were not large differences between cumulative biochar C
400 mineralization in aged versus unaged biochars. We observed an increase in biochar C mineralized
401 for 550CHEM compared to unaged biochar through the incubation period and a slight increase in
402 biochar C mineralization for 550PHY and 550BIO after about 400 hours after the start of
403 incubation, but the differences in means were not significant (Fig. 2). These observations were
404 consistent with trends in growth measurements on 550 °C biochar agar surfaces, where the average
405 surface growth was 43% greater for 550CHEM compared to 550UN but no difference in growth
406 was observed for 550BIO and 550PHY treatments (S.I. Fig. S2).
407
408 Biochar C mineralization across temperature and ageing treatments was significantly correlated
409 with elemental composition (Fig. 3) and surface chemistry (Fig. 4). The greatest changes in surface
410 and bulk chemistry were observed during physical ageing – specifically, we saw the greatest
411 increase in O/C ratio and carboxyl groups and the greatest loss of aromatic and aliphatic C in
412 350PHY. These changes were accompanied by significantly higher biochar mineralization
413 compared to unaged biochar. These correlations were notable across the full dataset for 350 °C
414 chars. We identified a significant positive correlation between the O/C ratio and cumulative
415 biochar C mineralized (R^2=0.778, $p<0.001$; Fig. 3) and between relative peak height of carboxylic
416 functional groups and cumulative biochar C mineralized (R^2=0.731, $p<0.001$ for 1701 cm^{-1};
417 R^2=0.37, p=0.021 for 1200 cm^{-1}; Fig. 4). Conversely, we identified a negative correlation between
418 aromatic C and cumulative biochar C mineralized (R^2 = 0.372, p=0.021 for 1593 cm^{-1}; R^2 = 0.464,
419 p=0.0073; for 810 cm^{-1}; Fig. 4) and between aliphatic C and cumulative biochar C mineralized (R^2

420 = 0.869, $p<0.001$ for 1413 cm^{-1}; $R^2 = 0.832$, $p<0.001$; for 2932 cm^{-1}; Fig. 4). These trends point to
421 two factors that may primarily be responsible for the increase in mineralization with ageing for
422 350°C biochars:

423 (i) *higher O/C ratio of aged biochar:* An increase in carboxylic and phenolic groups during
424 ageing could increase the O/C ratio of biochar, which makes it less stable, more
425 hydrophilic and more likely to be mineralized by microbes [12,66,72]. This surface-oxidized
426 biochar is easier to break down and could potentially facilitate the microbial metabolism
427 of ring structures that would ordinarily be highly recalcitrant [14,17,56].

428 (ii) *oxidation/transformation of surface aromatic carbon to aliphatic C:* Oxidative
429 transformation of aromatic C to linear alkyl-C and O-alkyl-C [63] could decrease ring
430 condensation and make carbon more susceptible to microbial breakdown. Further,
431 studies have documented breakdown and release of aromatic moieties in biochar to low
432 molecular-weight organic acids during ageing [73,74].

433

434

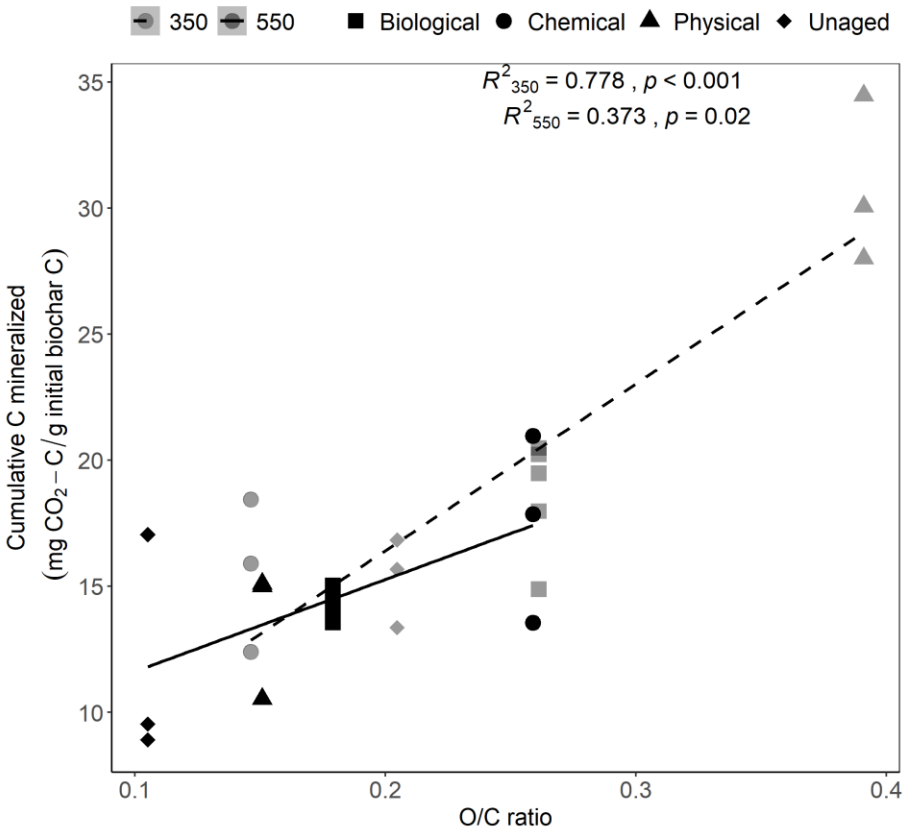

435

436 **Figure 3.** Relationship between cumulative biochar-C mineralized and molar O/C ratio. Shapes

437 indicate unaged, physically, chemically and biologically aged biochar samples produced at 350 °C

438 (light) and 550 °C (dark).

439

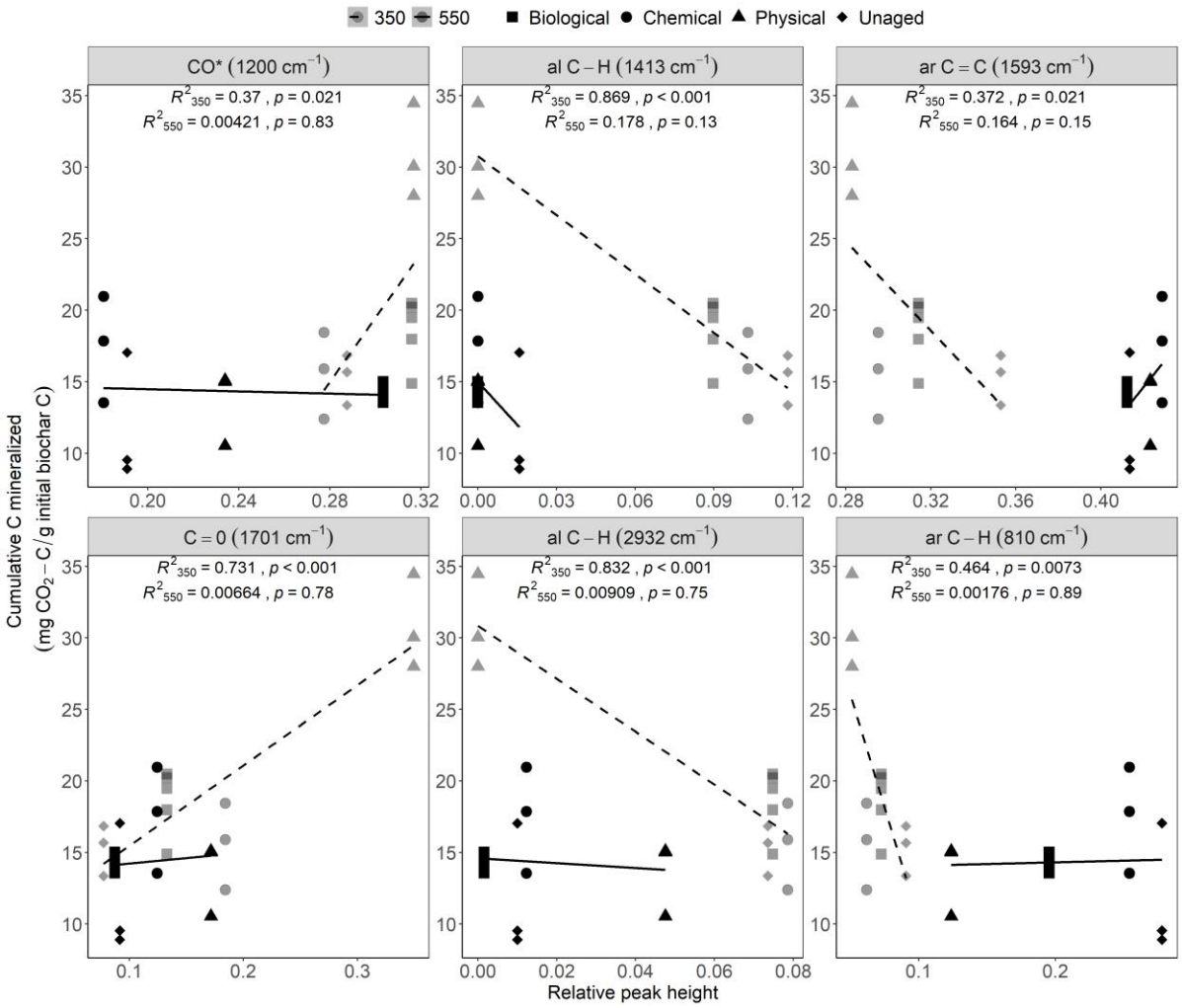

Figure 4. Relationship between cumulative biochar-C mineralized and FTIR spectra relative peak heights. Shapes indicate unaged, physically, chemically and biologically aged biochar samples produced at 350 °C (light) and 550 °C (dark). Panels indicate the peak names assigned to different functional groups at the given wavelength.

For the 550 °C chars, we identified a positive correlation between the O/C ratio and cumulative biochar C mineralized (R^2=0.373, p=0.02; Fig. 3) which suggests an increase in the mineralizability of biochar during ageing just as in the case of 350°C biochar. However, we were unable to identify any significant correlations between surface functional groups and cumulative

450 biochar C mineralized (Fig. 4), which is perhaps to be expected, due to the non-significant
451 differences in mineralization rates across 550 °C aged biochars. Even though increases in surface
452 oxidation and loss of some surface aromatic and aliphatic C groups were observed during ageing,
453 550 °C aged chars still retained more aromatic C and were less oxidized than 350 °C aged chars
454 as observed by measuring FTIR relative heights (S.I. Table S2). As a result, there is likely to be
455 less easily mineralizable C present in 550 °C biochars, even after ageing. This is in line with other
456 studies that have documented an inverse relationship between mineralization and aromatic fraction
457 in biochars [56,68]. This effect is potentially the primary reason we did not observe a significant
458 increase in biochar C mineralized for 550 °C chars during ageing despite observing changes in the
459 surface oxidation (Fig. 1a & Fig. 2).
460
461 This study provides evidence that higher O/C ratio and surface oxidation during ageing is likely
462 to accelerate biochar C mineralization by microbes. In particular, the surface oxidation of the
463 aromatic C groups has important implications for C management and cycling for both low
464 temperature biochars and naturally produced wildfire pyrogenic organic matter (PyOM). It has
465 been suggested that the chemical stability of natural wildfire PyOM produced at high temperatures
466 is more comparable to low temperature biochars as natural PyOM was found to consist of small
467 clusters of aromatic C units and not highly condensed polyaromatic structures [75–77]. Based on our
468 findings, the carbon in these PyOM materials could be more susceptible to surface oxidation and
469 C loss during ageing which could lead to increased mineralizability and thus decreased C storage
470 potential.
471

The ageing treatments used in this study were designed to simulate real world processes that occur naturally to biochars in soil. While it is not feasible to develop a scale to quantify the relative severity of our treatments compared to their expected severity in nature, our study highlights the role of abiotic factors like freeze-thaw-wet-dry processes in accelerating surface oxidation, which, in turn, increases the susceptibility of biochar to microbial degradation. There is a need to better understand the underlying mechanisms of surface oxidation in these processes and to design a more quantitative method to simulate ageing [34].

It is important to note that ageing and incubation of biochar was performed in the absence of soil (sand medium was used for physical ageing only), to control the processes of interest. However, we note that in soil systems, biochar-clay interactions, biochar-soil organic matter interactions as well as physical protection of biochar through aggregate formation are likely to affect both ageing of biochar and its interactions with microbes [58,78,79]. Further investigation into changes in bulk and surface properties associated with long term ageing of biochar in biochar amended soils could help in verification of laboratory biochar ageing and incubation studies as well as broaden our understanding of the potential of biochar as a C sink [34].

Supporting Information

FT-IR functional group peak assignments for biochar (Table S1); FTIR spectra relative peak heights (Table S2); Images of *Streptomyces* isolate growth on biochar- raw and processed using ImageJ (Figure S1); Comparison of *Streptomyces* isolate growth on aged and unaged biochar nutrient agar media (Figure S2); Details of biochar production and chemical analyses (Note S1);

494 Details of biochar nutrient media preparation (Note S2); Effect of ageing on pH (Note S3);
495 Elemental composition and surface chemistry of unaged biochar (Note S4).

496

497 **Author Contributions**

498 The authors confirm contribution to the paper as follows: study conception and design: NZ, TLW;
499 data collection: NZ, TDB; analysis and interpretation of results: NZ, TDB, TLW; draft manuscript
500 preparation: NZ; manuscript review and editing: NZ, TDB, TLW. All authors have reviewed the
501 results and have given approval to the final version of the manuscript.

502 **Funding sources**

503 This research was supported by the DOE Office of Science, Office of Biological and
504 Environmental Research (BER), grants no. DE-SC0020351 and no. DE-SC0016365.

505 **Notes**

506 The authors declare no competing financial interest.

507 **Acknowledgements**

508 This research was funded by the U.S. Department of Energy (DE-SC0020351; DE-SC0016365).
509 We thank Akio Enders for supplying the biochar that we used to isolate *Streptomyces* and for
510 assistance with biochar production. We are thankful to Kevin Panke-Buisse at USDA ARS,
511 Maggie Phillips at the Jackson Lab and Kim Sparks at the Cornell Stable Isotope Laboratory for
512 assistance with chemical analyses. Thanks to Jamie Woolet for isolating *Streptomyces* on biochar
513 and for all the technical assistance with the incubations. We also thank Monika Fischer and Neem
514 Patel for supplying the soil samples that we used during biological ageing.

References

(1) International Biochar Initiative. Standardized product definition and product testing guidelines for biochar that is used in soil. 2015.

(2) *Biochar for Environmental Management: Science, Technology and Implementation*, 2nd ed.; Johannes, L., Stephen, J., Eds.; Routledge: London, 2015.

(3) Schmidt, M. W. I.; Noack, A. G. Black carbon in soils and sediments: analysis, distribution, implications, and current challenges. *Global Biogeochem. Cycles* **2000**, *14* (3), 777–793.

(4) Woolf, D.; Amonette, J. E.; Street-Perrott, F. A.; Lehmann, J.; Joseph, S. Sustainable biochar to mitigate global climate change . *Nat. Commun.* **2010**, *1* (1), 56.

(5) Whitman, T.; Scholz, S. M.; Lehmann, J. Biochar projects for mitigating climate change: an investigation of critical methodology issues for carbon accounting. *Carbon Manag.* **2010**, *1* (1), 89–107.

(6) Whitman, T.; Hanley, K.; Enders, A.; Lehmann, J. Predicting pyrogenic organic matter mineralization from its initial properties and implications for carbon management. *Org. Geochem.* **2013**, *64*, 76–83.

(7) Campbell, J. L.; Sessions, J.; Smith, D.; Trippe, K. Potential carbon storage in biochar made from logging residue: basic principles and southern Oregon case studies. *PLoS One* **2018**, *13* (9), e0203475.

(8) Baldock, J.; Smernik, R. Chemical composition and bioavailability of thermally altered Pinus resinosa (Red pine) wood. *Org. Geochem.* **2002**, *33*, 1093–1109.

(9) Preston, C. M.; Schmidt, M. W. I. Black (pyrogenic) carbon: a synthesis of current knowledge and uncertainties with special consideration of boreal regions. *Biogeosciences* **2006**, *3* (4), 397–420.

(10) Nguyen, B. T.; Lehmann, J.; Hockaday, W. C.; Joseph, S.; Masiello, C. A. Temperature sensitivity of black carbon decomposition and oxidation. *Environ. Sci. Technol.* **2010**, *44* (9), 3324–3331.

(11) Keiluweit, M.; Nico, P. S.; Johnson, M. G.; Kleber, M. Dynamic molecular structure of plant biomass-derived black carbon (biochar). *Environ. Sci. Technol.* **2010**, *44* (4), 1247–1253.

(12) Spokas, K. A. Review of the stability of biochar in soils: predictability of O:C molar ratios. *Carbon Manag.* **2010**, *1* (2), 289–303.

(13) Enders, A.; Hanley, K.; Whitman, T.; Joseph, S.; Lehmann, J. Characterization of biochars to evaluate recalcitrance and agronomic performance. *Bioresour. Technol.* **2012**, *114*, 644–653.

(14) Cheng, C.-H.; Lehmann, J. Ageing of black carbon along a temperature gradient. *Chemosphere* **2009**, *75* (8), 1021–1027.

(15) Mukherjee, A.; Zimmerman, A. R.; Hamdan, R.; Cooper, W. T. Physicochemical changes in pyrogenic organic matter (biochar) after 15 months of field aging. *Solid Earth* **2014**, *5*, 693–704.

(16) Singh, B.; Fang, Y.; Johnston, C. T. A Fourier-Transform Infrared study of biochar aging in soils. *Soil Sci. Soc. Am. J.* **2016**, *80* (3), 613–622.

(17) Mia, S.; Dijkstra, F. A.; Singh, B. Chapter one - Long-term aging of biochar: a molecular understanding with agricultural and environmental implications. In *Advances in Agronomy*; Elsevier: Amsterdam, 2017; pp 1–51.

(18) Hale, S. E.; Hanley, K.; Lehmann, J.; Zimmerman, A. R.; Cornelissen, G. Effects of chemical, biological, and physical aging as well as soil addition on the sorption of pyrene to activated carbon and biochar. *Environ. Sci. Technol.* **2012**, *46* (4), 2479–2480.

(19) Xu, Z.; Xu, X.; Tsang, D. C. W.; Cao, X. Contrasting impacts of pre- and post-application aging of biochar on the immobilization of Cd in contaminated soils. *Environ. Pollut.* **2018**, *242* (Pt B), 1362–1370.

(20) Cao, Y.; Jing, Y.; Hao, H.; Wang, X. Changes in the physicochemical characteristics of peanut straw biochar after freeze-thaw and dry-wet aging treatments of the biomass. *BioResources* **2019**, *14* (2), 4329–4343.

(21) Huff, M. D.; Lee, J. W. Biochar-surface oxygenation with hydrogen peroxide. *J. Environ. Manage.* **2016**, *165*, 17–21.

(22) Gámiz, B.; Hall, K.; Spokas, K. A.; Cox, L. Understanding activation effects on low-temperature biochar for optimization of herbicide sorption. *Agronomy* **2019**, *9* (10), 588.

(23) Cross, A.; Sohi, S. P. A method for screening the relative long-term stability of biochar. *GCB Bioenergy* **2013**, *5*, 215–220.

(24) Kuzyakov, Y.; Subbotina, I.; Chen, H.; Bogomolova, I.; Xu, X. Black carbon decomposition and incorporation into soil microbial biomass estimated by 14C labeling. *Soil Biol. Biochem.* **2009**, *41* (2), 210–219.

577 (25) Kuzyakov, Y.; Bogomolova, I.; Glaser, B. Biochar stability in soil: decomposition during
578 eight years and transformation as assessed by compound-specific 14C analysis. *Soil Biol.*
579 *Biochem.* **2014**, *70*, 229–236.

580 (26) Santos, F.; Torn, M. S.; Bird, J. A. Biological degradation of pyrogenic organic matter in
581 temperate forest soils. *Soil Biol. Biochem.* **2012**, *51*, 115–124.

582 (27) Farrell, M.; Kuhn, T. K.; Macdonald, L. M.; Maddern, T. M.; Murphy, D. V; Hall, P. A.;
583 Singh, B. P.; Baumann, K.; Krull, E. S.; Baldock, J. A. Microbial utilisation of biochar-
584 derived carbon. *Sci. Total Environ.* **2013**, *465*, 288–297.

585 (28) Whitman, T.; Zhu, Z.; Lehmann, J. Carbon mineralizability determines interactive effects
586 on mineralization of pyrogenic organic matter and soil organic carbon. *Environ. Sci.*
587 *Technol.* **2014**, *48* (23), 13727–13734.

588 (29) Jones, D. L.; Edwards-Jones, G.; Murphy, D. V. Biochar mediated alterations in herbicide
589 breakdown and leaching in soil. *Soil Biol. Biochem.* **2011**, *43*, 804–813.

590 (30) Cheng, C.-H.; Lehmann, J.; Thies, J. E.; Burton, S. D.; Engelhard, M. H. Oxidation of black
591 carbon by biotic and abiotic processes. *Org. Geochem.* **2006**, *37* (11), 1477–1488.

592 (31) Liu, Z.; Demisie, W.; Zhang, M. Simulated degradation of biochar and its potential
593 environmental implications. *Environ. Pollut.* **2013**, *179*, 146–152.

594 (32) Spokas, K. Impact of biochar field aging on laboratory greenhouse gas production
595 potentials. *GCB Bioenergy* **2013**, *5*, 165–176.

596 (33) Liu, Z.; Zhu, M.; Wang, J.; Liu, X.; Guo, W.; Zheng, J.; Bian, R.; Wang, G.; Zhang, X.;
597 Cheng, K.; Liu, X.; Li, L.; Pan, G. The responses of soil organic carbon mineralization and

598 microbial communities to fresh and aged biochar soil amendments. *GCB Bioenergy* **2019**,
599 *11* (12), 1408–1420.

600 (34) Wang, L.; O'Connor, D.; Rinklebe, J.; Ok, Y. S.; Tsang, D. C. W.; Shen, Z.; Hou, D.
601 Biochar aging: mechanisms, physicochemical changes, assessment, and implications for
602 field applications. *Environ. Sci. Technol.* **2020**, *54* (23), 14797–14814.

603 (35) Güereña, D. T.; Lehmann, J.; Thies, J. E.; Enders, A.; Karanja, N.; Neufeldt, H. Partitioning
604 the contributions of biochar properties to enhanced biological nitrogen fixation in common
605 bean (Phaseolus vulgaris). *Biol. Fertil. soils* **2015**, *51* (4), 479–491.

606 (36) Biasutti, M.; Seager, R. Projected changes in US rainfall erosivity. *Hydrol. Earth Syst. Sci.*
607 **2015**, *19* (6), 2945–2961.

608 (37) Boswell, E. P.; Balster, N. J.; Bajcz, A. W.; Thompson, A. M. Soil aggregation returns to a
609 set point despite seasonal response to snow manipulation. *Geoderma* **2020**, *357*, 113954.

610 (38) Han, L.; Ro, K.; Wang, Y.; Sun, K.; Sun, H.; Libra, J.; Xing, B. Oxidation resistance of
611 biochars as a function of feedstock and pyrolysis condition. *Sci. Total Environ.* **2017**, *616–*
612 *617*, 335–344.

613 (39) Blodgett Forest Research Station | Berkeley Forests
614 https://forests.berkeley.edu/forests/blodgett.

615 (40) Stevenson, B. S.; Eichorst, S. A.; Wertz, J. T.; Schmidt, T. M.; Breznak, J. A. New strategies
616 for cultivation and detection of previously uncultured microbes. *Appl. Environ. Microbiol.*
617 **2004**, *70* (8), 4748–4755.

618 (41) Widdel, F.; Bak, F. Gram-negative mesophilic sulfate-reducing bacteria. In *The*

Prokaryotes; Balows, A., Trüper, H. G., Dworkin, M., Harder, W., Schleifer, K.-H., Eds.; Springer New York: New York, NY, 1992; pp 3352–3378.

(42) Galili, T. dendextend: an R package for visualizing, adjusting, and comparing trees of hierarchical clustering. *Bioinformatics* **2015**.

(43) Woolet, J.; Whitman, T. Pyrogenic organic matter effects on soil bacterial community composition. *Soil Biol. Biochem.* **2020**, *141*, 107678.

(44) Hartman, D. Perfecting your spread plate technique. *J. Microbiol. Biol. Educ.* **2011**, *12* (2), 204–205.

(45) Berry, T.; Creelman, C.; Nickerson, N.; Enders, A.; Whitman, T. An open-source, automated, gas sampling peripheral for laboratory incubation experiments. Manuscript submitted for publication 2020.

(46) Wickham, H.; Averick, M.; Bryan, J.; Chang, W.; McGowan, L. D.; Francois, R.; Grolemund, G.; Hayes, A.; Henry, L.; Hester, J.; Kuhn, M.; Pedersen, T. L.; Miller, E.; Bache, S. M.; Muller, K.; Ooms, J.; Robinson, D.; Seidel, D. P.; Spinu, V.; Takahashi, K.; Vaughan, D.; Wilke, C.; Woo, K.; Yutani, H. Welcome to the tidyverse. *J. Open Source Softw.* **2019**, *4* (43), 1686.

(47) Zeileis, A.; Grothendieck, G. zoo: S3 infrastructure for regular and irregular time series. *J. Stat. Softw.* **2005**, *14* (6), 1–27.

(48) Neuwirth, E. RColorBrewer: ColorBrewer palettes. 2014.

(49) Robinson, D.; Hayes, A. broom: convert statistical analysis objects into tidy tibbles. 2020.

639 (50) Wickham, H.; Francois, R.; Henry, L.; Muller, K. dplyr: a grammar of data manipulation.
640 2020.

641 (51) Wickham, H.; Henry, L. tidyr: tidy messy data. 2020.

642 (52) Wickham, H. *Ggplot2: Elegant Graphics for Data Analysis*; Springer-Verlag New York,
643 2016.

644 (53) Ram, K.; Wickham, H. wesanderson: a Wes Anderson palette generator. 2018.

645 (54) Schneider, C. A.; Rasband, W. S.; Eliceiri, K. W. NIH Image to ImageJ: 25 years of image
646 analysis. *Nat. Methods* **2012**, *9* (7), 671–675.

647 (55) Quan, G.; Fan, Q.; Zimmerman, A. R.; Sun, J.; Cui, L.; Wang, H.; Gao, B.; Yan, J. Effects
648 of laboratory biotic aging on the characteristics of biochar and its water-soluble organic
649 products. *J. Hazard. Mater.* **2020**, *382*, 121071.

650 (56) Bruun, E.; Hauggaard-Nielsen, H.; Ibrahim, N.; Egsgaard, H.; Ambus, P.; Jensen, P.; Dam-
651 Johansen, K. Influence of fast pyrolysis temperature on biochar labile fraction and short-
652 term carbon loss in a loamy soil. *Biomass Bioenergy* **2011**, *35* (3), 1182–1189.

653 (57) Tomczyk, A.; Sokołowska, Z.; Boguta, P. Biochar physicochemical properties: pyrolysis
654 temperature and feedstock kind effects. *Rev. Environ. Sci. Bio/Technology* **2020**, *19*, 191–
655 215.

656 (58) Singh, B. P.; Cowie, A. L.; Smernik, R. J. Biochar carbon stability in a clayey soil as a
657 function of feedstock and pyrolysis temperature. *Environ. Sci. Technol.* **2012**, *46* (21),
658 11770–11778.

659 (59) Crombie, K.; Mašek, O.; Sohi, S. P.; Brownsort, P.; Cross, A. The effect of pyrolysis
660 conditions on biochar stability as determined by three methods. *GCB Bioenergy* **2013**, *5* (2),
661 122–131.

662 (60) Zimmerman, A. R.; Ouyang, L. Priming of pyrogenic C (biochar) mineralization by
663 dissolved organic matter and vice versa. *Soil Biol. Biochem.* **2019**, *130*, 105–112.

664 (61) Glaser, B.; Lehmann, J.; Zech, W. Ameliorating physical and chemical properties of highly
665 weathered soils in the tropics with charcoal – a review. *Biol. Fertil. Soils* **2002**, *35* (4), 219–
666 230.

667 (62) Liang, B.; Lehmann, J.; Solomon, D.; Kinyangi, J.; Grossman, J.; O'Neill, B.; Skjemstad,
668 J. O.; Thies, J.; Luizão, F. J.; Petersen, J.; Neves, E. G. Black carbon increases cation
669 exchange capacity in soils. *Soil Sci. Soc. Am. J.* **2006**, *70* (5), 1719–1730.

670 (63) Yi, Q.; Liang, B.; Nan, Q.; Wang, H.; Zhang, W.; Wu, W. Temporal physicochemical
671 changes and transformation of biochar in a rice paddy: insights from a 9-year field
672 experiment. *Sci. Total Environ.* **2020**, *721*, 137670.

673 (64) Whitman, T.; Enders, A.; Lehmann, J. Pyrogenic carbon additions to soil counteract positive
674 priming of soil carbon mineralization by plants. *Soil Biol. Biochem.* **2014**, *73*, 33–41.

675 (65) Whitman, T.; Pepe-Ranney, C.; Enders, A.; Koechli, C.; Campbell, A.; Buckley, D. H.;
676 Lehmann, J. Dynamics of microbial community composition and soil organic carbon
677 mineralization in soil following addition of pyrogenic and fresh organic matter. *ISME J.*
678 **2016**, *10*, 2918–2930.

679 (66) Zimmerman, A. R. Abiotic and microbial oxidation of laboratory-produced black carbon

(biochar). *Environ. Sci. Technol.* **2010**, *44* (4), 1295–1301.

(67) Zimmerman, A.; Gao, B.; Ahn, M.-Y. Positive and negative carbon mineralization priming effects among a variety of biochar-amended soils. *Soil Biol. Biochem.* **2011**, *43*, 1169–1179.

(68) Dai, Z.; Barberán, A.; Li, Y.; Brookes, P. C.; Xu, J. Bacterial community composition associated with pyrogenic organic matter (biochar) varies with pyrolysis temperature and colonization environment. *mSphere* **2017**, *2* (2), e00085-17.

(69) Luo, Y.; Durenkamp, M.; De Nobili, M.; Lin, Q.; Brookes, P. C. Short term soil priming effects and the mineralisation of biochar following its incorporation to soils of different pH. *Soil Biol. Biochem.* **2011**, *43* (11), 2304–2314.

(70) Wiedemeier, D. B.; Abiven, S.; Hockaday, W. C.; Keiluweit, M.; Kleber, M.; Masiello, C. A.; McBeath, A. V; Nico, P. S.; Pyle, L. A.; Schneider, M. P. W.; Smernik, R. J.; Wiesenberg, G. L. B.; Schmidt, M. W. I. Aromaticity and degree of aromatic condensation of char. *Org. Geochem.* **2015**, *78*, 135–143.

(71) Wang, T.; Camps Arbestain, M.; Hedley, M. Predicting C aromaticity of biochars based on their elemental composition. *Org. Geochem.* **2013**, *62*, 1–6.

(72) Harvey, O. R.; Kuo, L.-J.; Zimmerman, A. R.; Louchouarn, P.; Amonette, J. E.; Herbert, B. E. An nndex-based approach to assessing recalcitrance and soil carbon sequestration potential of engineered black carbons (biochars). *Environ. Sci. Technol.* **2012**, *46* (3), 1415–1421.

(73) Yao, F. X.; Arbestain, M. C.; Virgel, S.; Blanco, F.; Arostegui, J.; Maciá-Agulló, J. A.; Macías, F. Simulated geochemical weathering of a mineral ash-rich biochar in a modified

soxhlet reactor. *Chemosphere* **2010**, *80* (7), 724–732.

(74) Hammes, K.; Smernik, R. J.; Skjemstad, J. O.; Schmidt, M. W. I. Characterisation and evaluation of reference materials for black carbon analysis using elemental composition, colour, BET surface area and 13C NMR spectroscopy. *Appl. Geochemistry* **2008**, *23* (8), 2113–2122.

(75) Knicker, H.; Hilscher, A.; González-Vila, F. J.; Almendros, G. A new conceptual model for the structural properties of char produced during vegetation fires. *Org. Geochem.* **2008**, *39*, 935–939.

(76) Schneider, M. P. W.; Pyle, L. A.; Clark, K. L.; Hockaday, W. C.; Masiello, C. A.; Schmidt, M. W. I. Toward a "molecular thermometer" to estimate the charring temperature of wildland charcoals derived from different biomass sources. *Environ. Sci. Technol.* **2013**, *47* (20), 11490–11495.

(77) Santín, C.; Doerr, S. H.; Merino, A.; Bucheli, T. D.; Bryant, R.; Ascough, P.; Gao, X.; Masiello, C. A. Carbon sequestration potential and physicochemical properties differ between wildfire charcoals and slow-pyrolysis biochars. *Sci. Rep.* **2017**, *7*, 11233.

(78) Cheng, C.-H.; Lehmann, J.; Engelhard, M. H. Natural oxidation of black carbon in soils: Changes in molecular form and surface charge along a climosequence. *Geochim. Cosmochim. Acta* **2008**, *72* (6), 1598–1610.

(79) Wang, J.; Xiong, Z.; Kuzyakov, Y. Biochar stability in soil: meta-analysis of decomposition and priming effects. *GCB Bioenergy* **2016**, *8* (3), 512–523.